www.ietdl.org

Published in IET Communications
Received on 1st February 2011
Revised on 21st April 2011
doi: 10.1049/iet-com.2011.0112

In Special Section: Photonic and Free Space Optics Networks

ISSN 1751-8628

Optimised non-uniform biasing technique for a high-speed optical router to achieve uniform semiconductor optical amplifier gain

W.P. Ng[1] *A.A. El Aziz*[1] *Z. Ghassemlooy*[1] *M.H. Aly*[2] *R. Ngah*[3]

[1]*Optical Communications Research Group, NCR Lab, Northumbria University, Newcastle upon Tyne, UK*
[2]*Arab Academy for Science and Technology and Maritime Transport, Alexandria, Egypt*
[3]*Wireless Communication Centre, Faculty of Electrical Engineering, Universiti Teknologi Malaysia, Skudai, Johor, Malaysia*
E-mail: wai-pang.ng@northumbria.ac.uk

Abstract: In this study, we propose applying non-uniform biasing current technique to improve the gain uniformity of the semiconductor optical amplifier (SOA) for high-speed optical routers. The output pulses will have high-gain deviation because of the high-speed input pulses and the slow SOA gain recovery, thus resulting in a high system power penalty. The theoretical SOA operation principle is demonstrated using a segmentation model that employs the rate and propagation equations with third-order gain coefficients. The impact of the bias current on the SOA gain responses owing to the input packet of 1 mW input Gaussian pulses at a wavelength of 1550 nm is analysed in order to optimise the proposed non-uniform bias current shape. The uniform and the optimised non-uniform bias current techniques are investigated in terms of the SOA gain uniformity and the average output power for high-speed data rates from 10 to 160 Gb/s. The impact of the average bias current applied to the SOA on the non-uniform shape is also investigated at all input data rates. Results obtained show a significant improvement in the gain standard deviation of 4.6, 6.3, 8.7, 10.1 and 10.2 dB for the data rates of 10, 20, 40, 80 and 160 Gb/s, respectively, when applying 150 mA average non-uniform biasing and these values reaches 15.2, 16.3, 17.7, 18 and 17.4 dB at 200 mA. The proposed technique also offers an increase in the average output power for the input pulses compared with uniform biasing.

1 Introduction

The use of wavelength division multiplexing (WDM) and optical time division multiplexing (OTDM) increases the overall capacity of the point-to-point optical fibre transmission systems. The development of high-capacity optical networks increased the demand of new optical devices that are able perform in almost all all-optical functions in order to overcome the speed and capacity bottleneck of optical–electrical–optical (OEO) conversion [1]. One of these key optical devices is a semiconductor optical amplifier (SOA) which is the most promising element for all-optical switching because of their small size, low switching energy non-linear characteristics and the seamless integration with other devices [2].

In order to avoid system penalties [3] arising from bit pattern dependencies and for more gain uniformity for high-bit-rate input signals, fast gain recovery is required in high-speed applications. The gain recovery of SOA is limited by the carrier lifetime, which itself depends on the applied bias current [1]. Different approaches have been used to speed-up the recovery time by changing the cavity length of the SOA or by changing the input pulse width [4]. Several research groups have reported theoretical and experimental results on externally injected SOAs [1, 5]. Investigation on non-uniform biasing has been reported in literatures using on and off impulses [6] and exponential shape current injections [7]. These investigations proposed to reduce the SOA switching time. However, the linearity of the output gain experienced by all input pulses has not been addressed in the current research. In [6], narrow current impulses were added with increasing amplitudes to the step signal. On the other hand, an exponential-shaped current injection was used in order to reduce the turn-on time delay in an SOA switch in [7]. This exponential biasing requires more energy to be applied to the SOA.

In this paper, we propose applying an optimised non-uniform current to the SOA for an input OTDM packet of Gaussian-shaped pulses in order to improve the SOA gain uniformity. We will theoretically investigate the SOA gain response owing to the input packet using uniform and non-uniform biasing currents techniques. The output gain uniformity and the average power for both techniques are compared at high-speed input data rates. The dependence of the optimised non-uniform shape on the average applied current will be investigated. The operation principle of the SOA is shown in the following section. Section 3 presents the mathematical analysis of the total gain and the change of the carrier density in terms of the rate and propagation equations. In Section 4, we optimise the bias current shape

and use it as an alternative to the uniform current in order to improve the SOA gain uniformity at high-speed data rates. The final section concludes the findings of the investigation.

2 SOA principle of operation

The SOA is an optoelectronic device that can amplify an input light signal under suitable operating conditions (see the SOA model in Fig. 1). An input signal enters the SOA from the input facet side through the active region where it achieves gain. Gain occurs when an external electric current is applied to supply the energy source to the active region [8]. The SOA is coated with input and output facets. The amplifier facets are reflective causing ripples in the gain spectrum [9]. Electrons acquire higher energy when the SOA is biased with a direct current. Therefore applying more bias current will result in a larger number of excited electrons in the conduction band.

Applying a short-duration input optical pulse into the SOA will result in stimulated emission leading to the signal amplification. The reduction of excited electrons (i.e. carrier density) in the conduction band will lead to a decreased SOA gain. This reduction is owing to the fact that the gain is proportional to the carrier population density. Moreover, this phenomenon will increase the active refractive index because of the non-linear refractive index being dependent on the carrier density [10].

The carrier non-equilibrium is governed mainly by the spectral hole burning effect [11]. The distribution recovers to its equilibrium state by the carrier–carrier scattering. Instantaneous mechanisms such as two-photon absorption and the optical Kerr effects [12] will then influence the SOA response. After few picoseconds, a quasi-equilibrium distribution will occur, owing to the carrier temperature relaxation process, followed by the carrier density recovery. The SOA gain recovery time is limited by the carriers' lifetime.

3 Theoretical model

We have developed a numerical model to analyse the bias current and its effect on the SOA gain. The model is based on position-dependent rate equations for the carrier density and the optical propagation equation in the forward-propagating direction for injected input pulses. Therefore the model accounts for a non-uniform carrier distribution. The complete rate equations in small segments in an SOA are iteratively calculated with third-order gain coefficients [13].

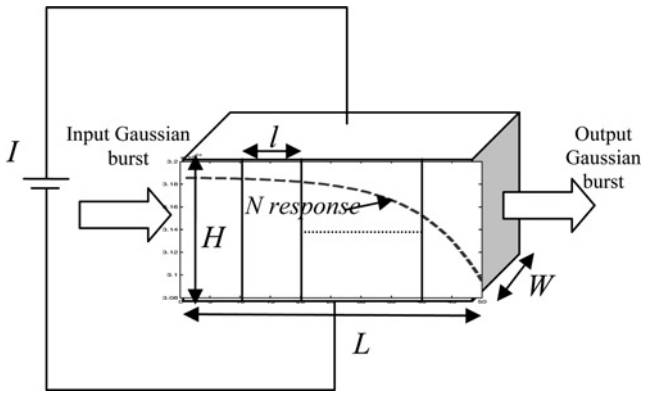

Fig. 1 *Segmentation model of the SOA device*

3.1 Rate equations

When light is injected into the SOA, changes occur in the carrier and photon densities within the active region that can be described using the rate equations. The gain medium of the amplifier is described by a third-order material gain coefficient g (per unit length), which is dependent on the carrier density N and the input pulse wavelength λ and is given by [14]

$$g = \frac{a_1 \times (N - N_O) - a_2 \times (\lambda - \lambda_N)^2 + a_3 \times (\lambda - \lambda_N)^3}{1 + (\varepsilon \times P_{\text{av}})} \tag{1}$$

where a_1 is the differential gain parameter, a_2 and a_3 are empirically determined constants that characterise the width and asymmetry of the gain profile, respectively. N_O is the carrier density at transparency point, λ_N is the wavelength at which the gain has a peak value, ε is the gain compression factor and P_{av} is the average output power. The peak gain wavelength is given by

$$\lambda_N = \lambda_O - [a_4 \times (N - N_O)] \tag{2}$$

where λ_O is the peak gain wavelength at transparency and a_4 is the empirical constant that shows the shift of the gain peak. The net gain coefficient is defined by

$$g_T = (\Gamma \times g) - \alpha_{\text{s}} \tag{3}$$

where Γ is the confinement factor which is the ratio of the light intensity within the active region to the sum of light intensity [8] and α_{s} is the internal waveguide scattering loss. The SOA gain achieved by an optical input signal at any given location z is given by

$$G = \text{e}^{g_T \times z} \tag{4}$$

Therefore the average output power over the length of the SOA L can be expressed by [15]

$$P_{\text{av}} = P_{\text{in}} \times \left(\frac{\text{e}^{g_T \times L} - 1}{g_T \times L} \right) \tag{5}$$

where P_{in} is the input pulse power. The rate of change of the carrier density within the active region of the device is given by

$$\frac{\text{d}N}{\text{d}t} = \frac{I}{q \times V} - [(A \times N) + (B \times N^2) + (C \times N^3)] - \frac{\Gamma \times g \times P_{\text{av}} \times L}{V \times h \times f} \tag{6}$$

where I is the SOA bias current, q is the electron charge, h is the Plank's constant and f is the light frequency. A is the surface and defect recombination coefficient while B and C are the radiative and Auger recombination coefficients, respectively. The active volume is determined by $V = L \times W \times H$ where W and H are the width and thickness of the active region, respectively.

3.2 Propagation equation

The SOA is assumed to have a negligible reflectivity at the end facets, so the reflected waves are omitted. The propagation equation for the forward light is given by [14]

$$\frac{dP_{in}}{dz} = [(\Gamma \times g) - \alpha_s] \times P_{in} \quad (7)$$

4 Segmentation model

This paper uses a segmentation model employing the rate and propagation equations presented in Section 3 [16]. These equations are adopted to investigate the gain of the SOA and the uniformity of the emerging output pulses using Matlab^{TM}.

Fig. 1 shows the reduction of N owing to the input pulse propagation through all segments of the SOA segmentation model. This model presents a bulk homogeneously broadened travelling-wave-type SOA divided into 50 equal segments, and the input pulse is single mode with narrow linewidths. The carrier density is assumed to be constant within each segment. However, the carrier density and the signal power changes from segment-to-segment depending on the input power and the carrier density of the previous segment.

Fifty segments were chosen to accurately investigate the effect of the input power on the change in the carrier density and the signal gain along the SOA for data rate up to 160 Gb/s. The SOA parameters implemented are obtained from [8, 14] and are given in Table 1.

In this paper, the input pulse to the SOA model is a Gaussian pulse with a full-wave-half-maximum (FWHM) of 1.167 ps and peak power of 1 mW. All the signal power is coupled directly into the SOA. The reason a short pulse of >1 ps pulse width is chosen as the input pulse is because at pulses <1 ps intraband relaxation processes are not sufficiently fast to instantaneously replenish the depleted carriers owing to amplification in the energy range corresponding to the pulse spectrum (spectral hole burning). If the average energy of the hole is lower than that of the initial state, the result is a rise in the average carrier temperature. The carrier-heating component becomes non-negligible as the pulse width approaches 1 ps [17].

Table 1 Physical parameters of the SOA

Parameter	Value
carrier density at transparency (N_O)	$1.4 \times 10^{24}/m^3$
wavelength at transparency (λ_O)	1605 nm
initial carrier density (N_i)	$3 \times 10^{24}/m^3$
signal wavelength (λ)	1550 nm
internal waveguide scattering loss (α_s)	$40 \times 10^2/m$
differential gain (a_1)	$2.78 \times 10^{-20}\ m^2$
gain constant (a_2)	$7.4 \times 10^{18}/m^3$
gain constant (a_3)	$3.155 \times 10^{25}/m^4$
gain peak shift coefficient (a_4)	$3 \times 10^{-32}\ m^4$
SOA length (L)	500 μm
SOA width (W)	3 μm
SOA height (H)	80 nm
confinement factor (Γ)	0.3
surface and defect recombination coefficient (A)	$3.6 \times 10^8/s$
radiative recombinassions coefficient (B)	$5.6 \times 10^{-16}\ m^3/s$
Auger recombination coefficient (C)	$3 \times 10^{-41}\ m^6/s$
gain compression factor (ε)	0.2/ W

5 Results and discussion

In order to understand the effect of the bias current and N rate of change (i.e. dN/dt) on the gain profile and SOA gain uniformity, a number of successive pulses are required to propagate along the SOA active region. Therefore a packet of identical Gaussian pulses is applied to the SOA at 1550 nm. The packet consists of ten pulses of 1 mW peak power and these pulses are separated by 100 ps (10 Gb/s) to fill a packet duration t_p of 1 ns. The gain response of the SOA when the packet is launched into the active region is displayed in Fig. 2. The rapid increase in the gain reaching a steady-state value within $t_{bias} \sim 1$ ns is because of the SOA biasing. A large quantity of electrons in the valence band will gain enough energy to overcome the energy gap, which increases N in the conduction band and hence the SOA total gain.

When the first pulse in the packet enters the SOA at $t \sim 3$ ns, sudden gain depletion occurs as a result of the interaction of the incident photons with excited electrons from the conduction band. This depletion takes place during the pulse propagation along the SOA lasting 5.83 ps. Owing to the slow recovery of the SOA gain, following the exodus of the first pulse, the next pulse enters the SOA prior to its full gain recovery. A further gain depletion is introduced because of the second pulse. This process continues until the last pulse exits the SOA.

In order for all pulses to accomplish the same gain, all the pulses should experience the same gain depletion. It is apparent from Fig. 2 that the gain reduction reaches different levels from one pulse to another (i.e. the gain depletion envelope is not uniform). Fig. 2 also shows that by applying a packet with more pulses, that is, more than ten pulses, the variation of gain depletion is negligible. Therefore there is no significant difference when injecting more than ten pulses in the current investigation. The applied bias current controls the number of excited electrons in the conduction band and hence the SOA gain. For that reason, in order for all pulses to achieve the same output gain, bias current characteristics are used so that these pulses enter the SOA at the same

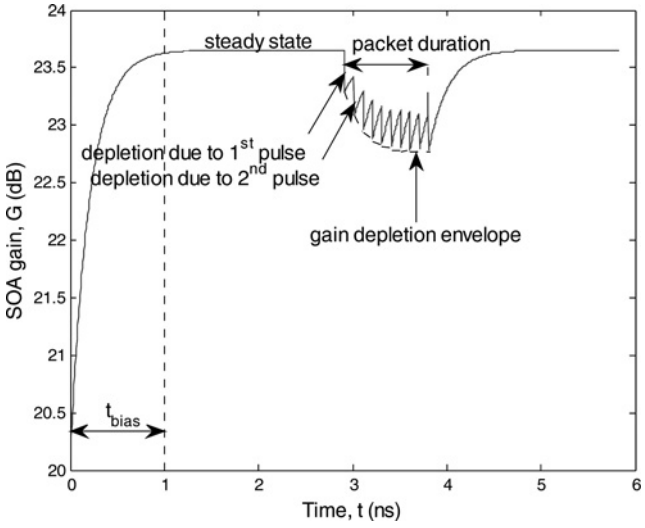

Fig. 2 *SOA gain response to a packet of successive 10 Gaussian pulses*

doi: 10.1049/iet-com.2011.0112

carrier density. Based on the direct temporal relationship of the bias current on the SOA gain shown in (6), we propose applying a non-uniform bias current to the SOA, where each Gaussian pulse enters the SOA at a different biasing value in order to improve the output gain uniformity. Consequently, in order to optimise the non-uniform bias current shape that would achieve the best gain uniformity, we investigate the SOA gain response of all the input pulses for a range of bias current values (see Fig. 3). From Fig. 3, one can see that the same gain (i.e. uniform output gain) can be achieved by the input pulses at different bias current values. However, it is important for the non-uniform bias current applied to the SOA to have an average value equivalent to the uniform bias current in order to maintain the same power used in both cases. For 10 Gb/s input data rate, this uniform output gain condition occurs at $G_m = 23.02$ dB (horizontal dashed line in Fig. 3). This gain value intersects with all pulses at different biasing values while maintaining an average bias current $I_{av} = 50$ mA where I oscillates between the minimum, I_{min}, and maximum, I_{max}, bias currents corresponding to the first and tenth pulses, respectively. The appropriate response of the non-uniform bias current should be inversely proportional to the SOA gain depletion envelope shown in Fig. 2. As a result, the proposed optimised non-uniform biasing shape at 10 Gb/s input data rate is shown in Fig. 4. The bias current cycle (repetition rate) covers the packet duration (i.e. 1 ns which is only 10% of the respective input data rate) and varies between 148.3 and 151.7 mA.

In this paper, we have adopted a bit pattern of all '1's in the simulation because this pattern will give the least recovery time for the SOA, thus resulting in the worst-case scenario for SOA gain depletion. The all '1's sequence is also a commonly used bit pattern in optical applications employing polarisation modulation techniques such as, SOA-based ultrafast all-optical switches [18, 19].

In order to measure the gain uniformity of the output pulses, the gain standard deviation is introduced, which is given by

$$\sigma = 10\log\left(\sqrt{\frac{1}{\mathrm{np}}\sum_{x=1}^{\mathrm{np}}(G_x - G_{\mathrm{av}})^2}\right) \tag{8}$$

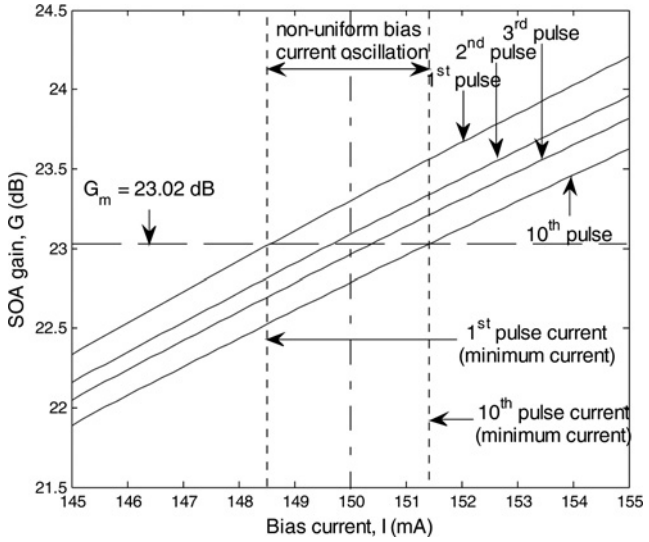

Fig. 3 *SOA gain response of all pulses within the packet to the uniform bias current*

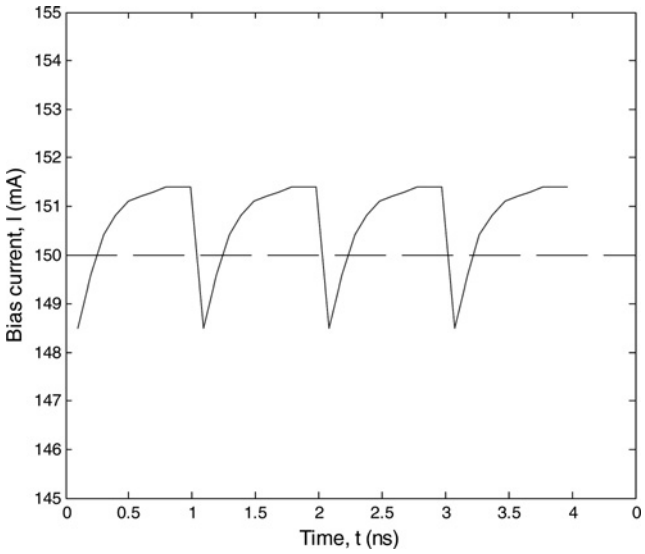

Fig. 4 *Optimised non-uniform bias current for input packet at 10 Gb/s*

where np is the number of successive input pulses within the packet launched into the SOA, G_x is the gain achieved by each input pulse and G_{av} is the average gain of all the pulses.

Comparing the gain uniformity of the SOA when biased with uniform and the proposed non-uniform bias currents, a significant improvement of 4.6 dB is achieved using the non-uniform biasing technique. It was highlighted earlier in this section that there is no vital need to apply more than 10 input pulses in the investigation; however, at data rates >10 Gb/s, the variations of gain depletion after the tenth pulse cannot be neglected. The injection of more number of input pulses at each higher data rate is necessary. Therefore in the following investigation, the number of input pulses per packet is increased at each data rate maintaining the packet duration of 1 ns. The input OTDM packet with different time separations, of 50, 25, 12.5 and 6.25 ps is launched to the SOA for 20, 40, 80 and 160 Gb/s, respectively. The change in the input pulses rate has a direct impact on the SOA total gain and, therefore, the gain uniformity. For all data rates, the depletion in the SOA gains because of the propagation of the first pulse of the input packet is similar; however, the time available for the gain to recover after the departure of the first pulse from the SOA is halved in each case. Therefore the second input pulse enters the SOA at a lower gain level (compared with lower data rate), and results in further gain depletion.

In order to understand this impact, the SOA gain response when a 1 ns packet of 20 Gaussian pulses at 20 Gb/s is applied to the SOA is displayed in Fig. 5. The figure shows the further depletion of SOA gain after the 10th pulse and it is clear that applying more than 20 pulses does not affect the gain depletion envelope. The same approach to optimise the non-uniform bias current (see Fig. 3) is employed for the 20 pulses packet. A reduction of 6.3 dB in σ is achieved employing the proposed biasing technique.

The shapes of the periodic 1 Gb/s biasing currents corresponding to the 20, 40, 80 and 160 Gb/s input packets are plotted in Figs. 6*a*–*d*, respectively. Fig. 6 shows that the optimised non-uniform current fluctuates within a higher range at higher data rates. These current fluctuation ranges are 6, 12.6, 22 and 35.6 mA at 20, 40 80 and 160 Gb/s, respectively, maintaining $I_{av} = 150$ mA.

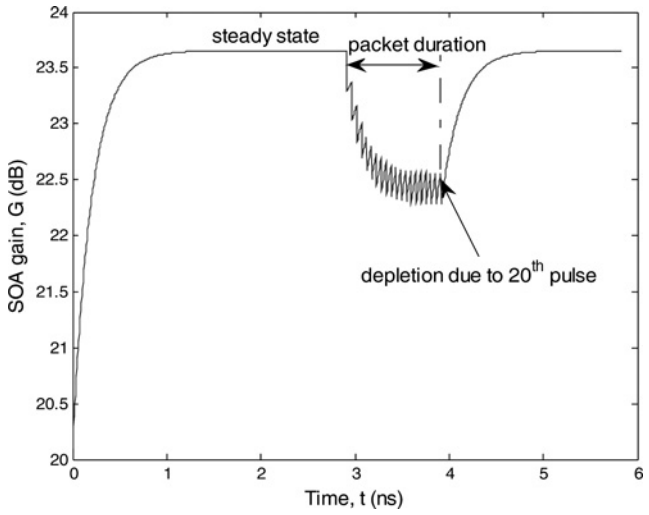

Fig. 5 *SOA gain response to a packet of successive 20 Gaussian pulses*

It is evident from Fig. 6 that biasing shapes at higher input rates have steeper slope to reach the maximum current value. This response refers to the slope of the gain depletion envelope of the first few pulses of the input packet. The reason for the steep slope at higher rates is because of the limited recovery time.

Based on the results obtained so far and the rate and propagation equations from Section 3, we have derived a general equation for the optimised non-uniform biasing shape at any input data rate and for any number of pulses which is given by

$$I = \frac{q \times V}{(2t_{\text{int}} + t_{\text{sep}})} \times \left[\frac{1}{\Gamma \times a_1 \times L} \ln\left[\frac{G_{\text{np}}}{G_{\text{ss}}}\right] + t_{\text{int}}\left(D_1 + \sum_{i=1}^{\text{np}-1} D_2 \frac{t_{\text{sep}}}{t_{\text{int}}} + \sum_{x=1}^{\text{np}} D_3\right)\right] \tag{9}$$

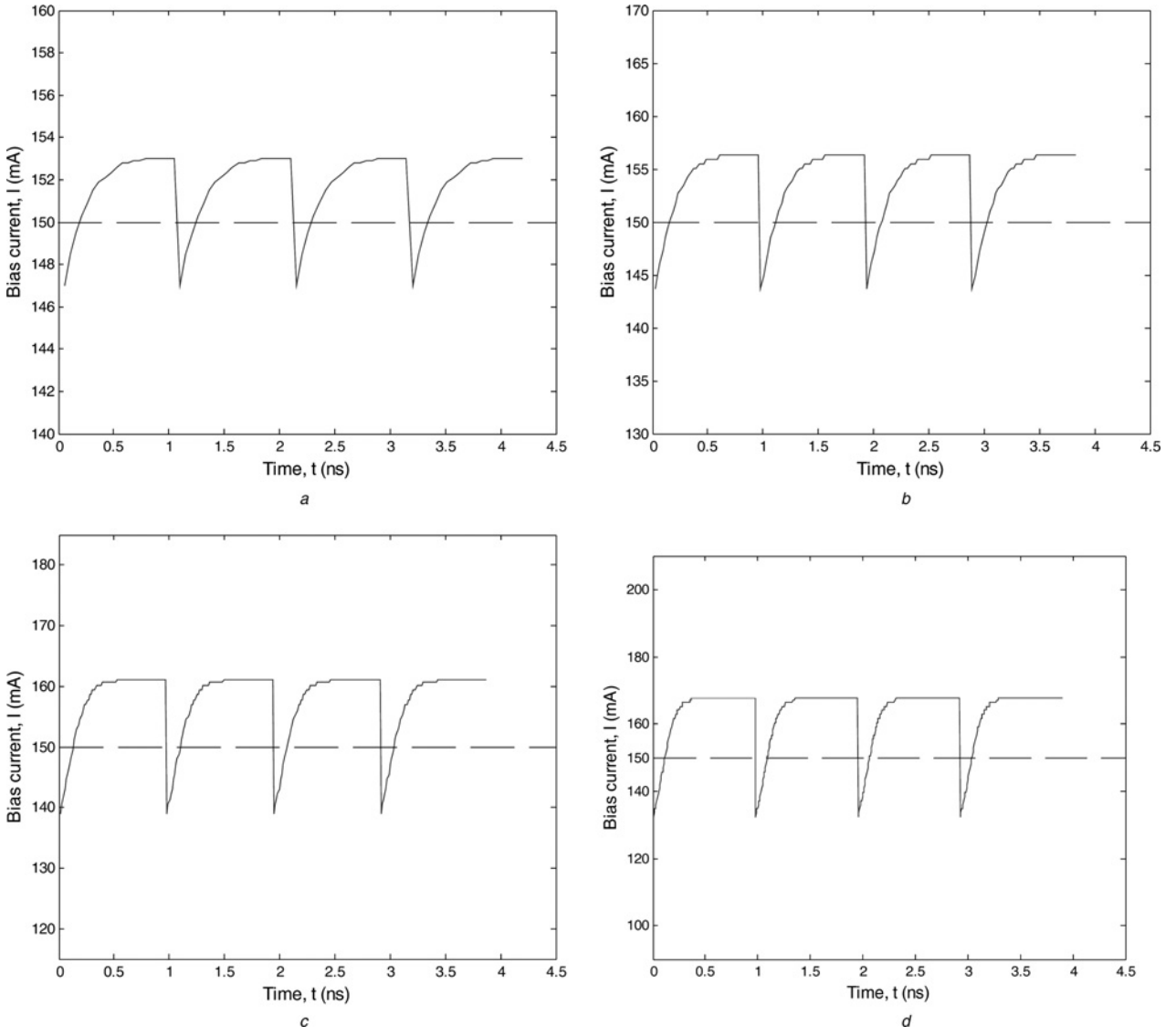

Fig. 6 *Optimised non-uniform bias current for input packet at*

a 20 Gb/s
b 40 Gb/s
c 80 Gb/s
d 160 Gb/s

doi: 10.1049/iet-com.2011.0112

where

$$D_1 = (A \times N_{ss} + B \times N_{ss}^2 + C \times N_{ss}^3) + \frac{\Gamma \times g_{ss} \times L \times P_{av1}}{V \times h \times f} \quad (10)$$

$$D_2 = (A \times N_i + B \times N_i^2 + C \times N_i^3) \quad (11)$$

$$D_3 = (A \times N_x + B \times N_x^2 + C \times N_x^3) + \left(\frac{\Gamma \times g_x \times L \times P_{avi}}{V \times h \times f}\right) \quad (12)$$

where t_{int} and t_{sep} are the time propagation of the pulse through the SOA (i.e. 5.83 ps) and the pulses separation time, respectively. G_{np} and G_{ss} are the SOA gains of the last pulse and at steady-state condition (i.e. before the entry of any pulse), respectively. N_{ss} and g_{ss} are the carrier density and gain coefficient at the steady-state value, respectively, whereas P_{av1} is the average power of the first pulse.

For the non-uniform technique, the maximum current value of the biasing shape should not exceed the practical SOA biasing limit of 300–400 mA [20]. This paper focuses on the 300 mA as the maximum (boundary) current limit for safe SOA operation. Therefore further investigations are carried out for higher I_{av}, that is, 200 and 250 mA at all data rates to find the boundary condition for the proposed technique. Results obtained show that in case of maintaining $I_{av} = 200$ mA, the I_{max} for the optimised biasing shapes are 206.7, 213, 224, 235.1 and 247.8 mA at 10, 20, 40, 80 and 160 Gb/s, respectively. On the other hand, for $I_{av} = 250$ mA, the I_{max} values are beyond 300 mA at 80 and 160 Gb/s. Nevertheless, the SOA gain uniformity is improved employing the non-uniform bias current in all cases.

The gain standard deviations for the packets at all data rates for $I_{av} = 150$ and 200 mA are measured using uniform and non-uniform biasing in order to distinguish the improvement of the SOA gain uniformity. The advantage of using the non-uniform technique over uniform biasing can be seen in Fig. 7. The figure depicts a bar chart of the σ improvement when the uniform bias current is replaced by the proposed technique at $I_{av} = 150$ and 200 mA for all rates. At higher input rates, more improvement in the SOA gain uniformity is achieved. Fig. 7 also shows that fluctuation of σ improvement is less perturbed at rates >40 Gb/s for both I_{av} cases. The reason for the small difference in σ improvement at higher rates is the shorter time spacing between input pulses. In case of using the non-uniform biasing technique, the average σ improvements are 8 and 16.9 dB for 150 and 200 mA I_{av}, respectively, at all the data rates investigated.

This paper also presents another key advantage of employing the non-uniform current for biasing the SOA which is the higher average output power. Although both biasing techniques supply the same power to the SOA, the proposed non-uniform technique offers higher-power amplifications for the input pulses. Fig. 8 introduces the increase in the average output peak power P_{poav} for using optimised non-uniform biasing instead of the uniform current at 150 and 200 mA I_{av}.

Fig. 8 shows that biasing the SOA with the proposed non-uniform current technique amplify the input pulses with higher power regardless of the pulses speed rate. The reason for such response is because of the continuous saturation in case of uniform biasing while the non-uniform technique allows gain recovery. Fig. 8 confirms the higher increase in P_{poav} at 200 mA I_{av} for all rates. The maximum increase in P_{poav} of 50.5 mW appears at 40 Gb/s maintaining $I_{av} = 200$ mA.

It is of interest to measure the impact of the non-uniform biasing technique on other optical applications that use random bit patterns. For that reason, we have applied input packets with the same random bit sequence to SOA biased with both techniques at all data rates.

Fig. 9 shows that σ is similar for both cases. However, the proposed technique improves (i.e. increases) the average output power of the packet regardless of the data rate or the average biasing current. The P_{poav} comparison between both biasing currents can be seen in Fig. 10 at I_{av} of 150 and 200 mA. Results show that applying input packets with random sequence results in higher P_{poav} achievements

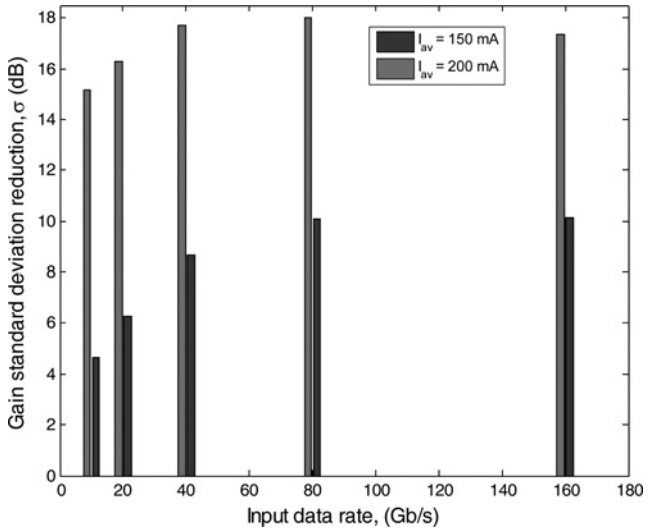

Fig. 7 *Gain standard deviation reduction employing the non-uniform bias current as a replacement of the uniform current for all '1's bit pattern packet*

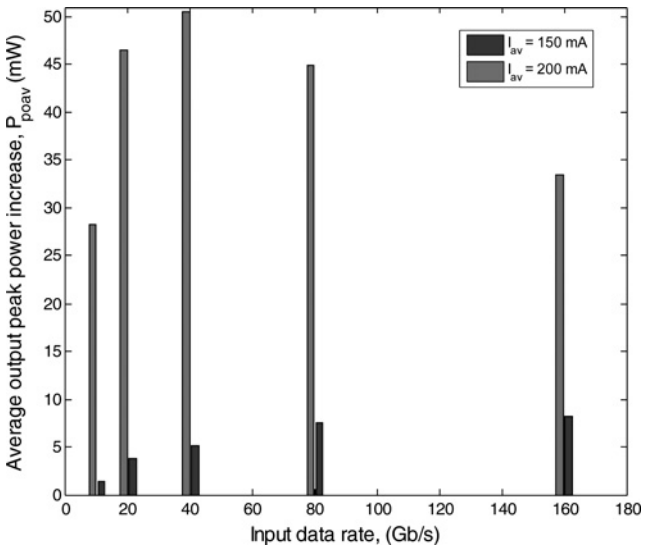

Fig. 8 *Average output peak power increase employing the non-uniform bias current as a replacement of the uniform current for all '1's bit pattern packet*

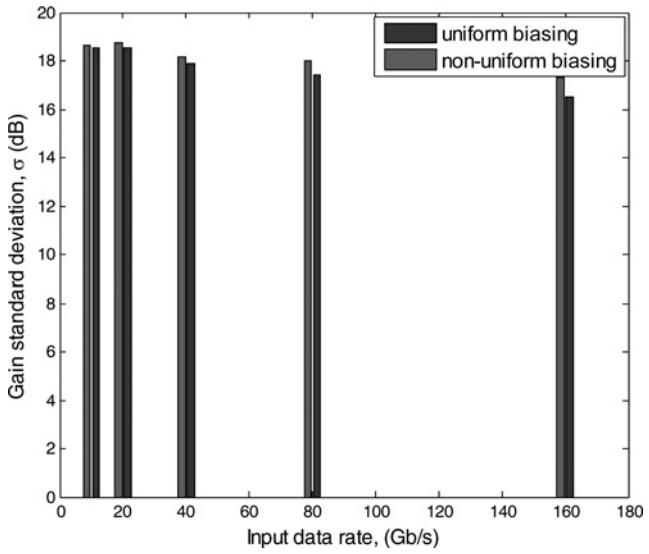

Fig. 9 *Comparison of gain standard deviation between uniform and non-uniform biasing techniques for random bit sequence packet*

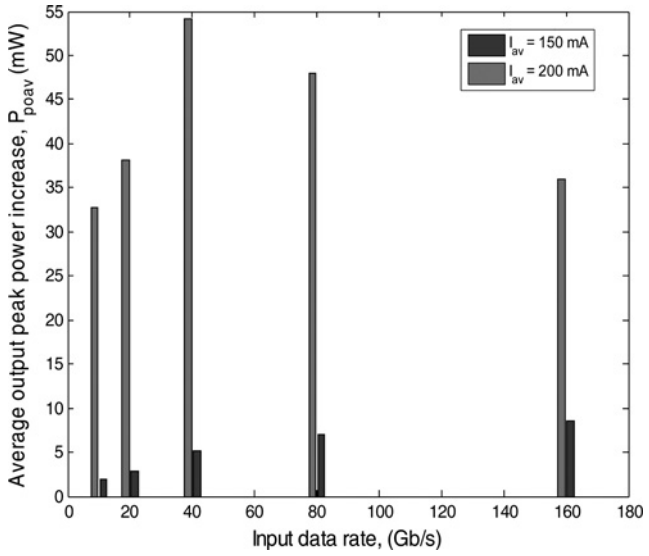

Fig. 10 *Average output peak power increase employing the non-uniform bias current as a replacement of the uniform current for random bit sequence packet*

compared with all '1's sequence at all input data rates (see Fig. 8).

6 Conclusions

This paper proposed an optimised non-uniform current shape to bias the SOA which was able to enhance the SOA gain uniformity at high-speed data rates. In this paper a gain standard deviation equation is introduced in order to measure the SOA gain uniformity. The carrier density and corresponding SOA gain uniformity dependence on the applied bias current are analysed. Accordingly, we have optimised a biasing shape for the SOA in order to linearise the gain of the input pulses. An SOA non-uniform bias current equation is proposed for the first time to optimise the gain uniformity at any input data rate and for any number of pulses. The optimised shape can be practically generated at 1 Gb/s and the practical results will be addressed in the next stage of this research.

The paper compared the uniform bias current to the non-uniform biasing technique for the same input packet to highlight the advantages of employing the proposed technique. The SOA gain uniformity resulted in significant improvement of the gain standard deviation (i.e. lower σ) at all investigated data rates. An enhancement of 4.6, 6.3, 8.7, 10.1 and 10.2 dB in the SOA gain uniformity when biased with the proposed current is achieved at input rates of 10, 20, 40, 80 and 160 Gb/s, respectively, for 150 mA average current. On the other hand, these values reach 15.2, 16.3, 17.7, 18 and 17.4 dB at 200 mA. The obtained results show average improvements of 8 and 16.9 dB for 150 and 200 mA I_{av}, respectively, at data rates investigated. The paper also investigated the average output power of the pulses between both biasing techniques. The optimised non-uniform current offered higher power amplifications for the input pulses regardless of the packet bit rate or sequence. The boundaries of the proposed technique are studied regarding the maximum current limit that should be reached by the non-uniform shape. The paper showed that the average output power will improve employing the proposed non-uniform biasing technique regardless of the input bit pattern while the gain uniformity will either show improvement or remain unaffected.

7 References

1 Pleumeekers, J.L., Kauer, M., Dreyer, K., *et al.*: 'Acceleration of gain recovery in semiconductor optical amplifiers by optical injection near transparency wavelength', *IEEE Photonics Technol. Lett.*, 2002, **14**, pp. 12–14

2 Tangdiongga, E., Liu, Y., Waardt, H., Khoe, G., Koonen, A., Dorren, H.: 'All-optical demultiplexing of 640 to 40 Gbits/s using filtered chirp of a semiconductor optical amplifier', *Opt. Lett.*, 2007, **32**, pp. 835–837

3 Pan, Z., Yang, H., Zhu, Z., *et al.*: 'Demonstration of variable-length packet contention resolution and packet forwarding in an optical-label switching router', *IEEE Photonic Technol. Lett.*, 2004, **16**, pp. 1772–1774

4 Ju, H., Zhang, S., Lenstra, D., *et al.*: 'SOA-based all-optical switch with subpicosecond full recovery', *Opt. Express*, 2005, **13**, pp. 942–947

5 Hessler, T.P., Dupertuis, M.-A., Deveaud, B., Emery, J.-Y., Dagens, B.: 'Optical speedup at transparency of the gain recovery', *Appl. Phys. B*, 2002, **81**, p. 3119

6 Gallep, C.M., Conforti, E.: 'Reduction of semiconductor optical amplifier switching times by preimpulse step-injected current technique', *IEEE Photonic Technol. Lett.*, 2002, **14**, pp. 902–904

7 Lee, M.H., Shin, S.M., Han, S.K.: 'Wavelength-converting optical space switch using a semiconductor-optical-amplifier-based Mach-Zehnder interferometer', *Opt. Eng.*, 2000, **39**, pp. 3255–3259

8 Connelly, M.: 'Semiconductor optical amplifiers' (Springer-Verlag, New York, 2002)

9 Keiser, G.: 'Optical fiber communication' (McGraw-Hill, Singapore, 2000)

10 Eiselt, M., Pieper, W., Weber, H.: 'SLALOM: semiconductor laser amplifier in a loop mirror', *IEEE J. Lightwave Technol.*, 1995, **13**, pp. 2099–2112

11 Guo, L., Connelly, M.: 'All-optical AND gate with improved extinction ratio using signal induced nonlinearities in a bulk semiconductor optical amplifier', *Opt. Express*, 2006, **14**, pp. 2938–2943

12 Agrawal, G.: 'Nonlinear fiber optics' (Academic Press, San Diego, USA, 1995, 2nd edn.)

13 Mendoza-Alvarez, J., Coldren, L., Alping, A., *et al.*: 'Analysis of depletion edge translation lightwave modulators', *IEEE J. Lightwave Technol.*, 1988, **6**, pp. 793–807

14 Wang, H., Wu, J., Lin, J.: 'Studies on the material transparent light in semiconductor optical amplifiers', *J. Opt. A*, 2005, **7**, pp. 479–492

15 VPI systems: 'VPI transmission maker and VPI component maker: photonic modules reference manual', 2001

16 Connelly, M.J.: 'Wideband semiconductor optical amplifier steady-state numerical model', *IEEE J. Quantum Electron.*, 2001, **37**, pp. 439–447

doi: 10.1049/iet-com.2011.0112

17 Tajima, K., Nakamura, S., Ueno, Y.: 'semiconductor nonlinearities for ultrafast all-optical gating', *Meas. Sci. Technol.*, 2002, **13**, pp. 1692–1697
18 Calvani, R., Caponi, R., Delpiano, F., Marone, G.: 'An experiment of optical heterodyne transmission with polarization modulation at 140 Mbit/s bitrate and 1550 nm wavelength'. Global Telecommunications Conf., 1991, GLOBECOM'91, Countdown to the New Millennium: Featuring a Mini-Theme on Personal Communications Services, 1991, vol. 3, pp. 1587–1591
19 Xinhui, Z., Yong, Y., Yunxu, S., Chao, L.: 'Circle polarization shift keying with direct detection for free-space optical communication', *IEEE/OSA J. Opt. Commun. Network.*, 2009, **1**, pp. 307–312
20 CIP Technologies: 'Quad 40 Gb/s 2R optical regenerator: preliminary datasheet', Rev G, accessed 16 October 2011